



ELSEVIER

29 August 1997

---

---

**CHEMICAL  
PHYSICS  
LETTERS**

---

---

Chemical Physics Letters 275 (1997) 127–136

# Quantum dynamics following electron photodetachment in the $I^-Ar_2$ complex. How good are the new separable and non-separable simulation methods?

Pavel Jungwirth<sup>a</sup>, Burkhard Schmidt<sup>b</sup><sup>a</sup> J. Heyrovský Institute of Physical Chemistry, Academy of Sciences of the Czech Republic, Dolejškova 3, 18223 Prague 8, Czech Republic<sup>b</sup> Institut für Physikalische und Theoretische Chemie, Freie Universität Berlin, Takustr. 3, 14195 Berlin, Germany

Received 24 April 1997; in final form 2 June 1997

---

## Abstract

The process of electron photodetachment in the  $I^-Ar_2$  cluster is chosen for testing new approximate quantum dynamical methods – the classical separable potential (CSP) approach and its configuration interaction (CI-CSP) extension. The results are encouraging in the sense of a quantitative agreement between the CSP and established time-dependent self-consistent field schemes, and in the fact that the inclusion of correlations via the CI-CSP approach brings the results significantly closer to exact ones. These findings justify applying the new methods to fast dynamical processes in moderately quantal large polyatomic systems, where other approaches become computationally demanding or unfeasible. © 1997 Elsevier Science B.V.

---

## 1. Introduction

Molecular dynamics (MD) techniques have proven to be useful tools in elucidating the nature of physical and chemical processes in atomic and molecular systems [1,2]. Despite the fact that quantum effects often have a significant influence on the nuclear dynamics and observed spectra, simulations are in most cases carried out within the classical *ansatz*. The reason for this is merely technical – while classical MD simulations for systems up to  $10^4$  atoms are now common, precise state-of-the-art quantum dynamical (QD) calculations are limited to diatomics, triatomics and, with tremendous effort, to tetraatomics. These numerically exact grid, discrete variable representation (DVR) or basis set QD methods [3–8] scale exponentially with system size, and it is therefore unlikely that they will soon be applicable to large chemically relevant systems.

Not to give up on the description of quantum effects in polyatomics connected, for example, with zero point motions, tunneling, non-adiabatic interactions with electronic motions or on correct spectra modeling, inevitably means pursuing approximate approaches. It is beyond the scope of this Letter to mention them all, in the following we concentrate on methods based on the separable (Hartree) approximation. Under the assumption that the total vibrational wavepacket can be approximated by a product of single mode terms the coupled multidimensional problem reduces to a set of one-dimensional Schrödinger equations indirectly coupled via effective time-dependent one-dimensional Hamiltonians. This time-dependent self-consistent field (TDSCF)

method [9–11] can also serve as a basis for configuration interaction (CI-TDSCF) and multi-configuration (MCTD SCF) techniques [12–17] where a sum of separable functions with variationally optimized coefficients better approximates the exact wavepacket.

The computational bottlenecks of the TDSCF method are the multidimensional numerical quadratures connected with the evaluation of effective one-dimensional potentials. Recently, we proposed a classical separable potential (CSP) method [18] where these terms are evaluated as weighted averages over auxiliary classical trajectories, which sped up the calculation by orders of magnitude and allowed quantum dynamical simulations of systems with more than one hundred degrees of freedom [19]. In the last months, the CSP method has also been extended in the direction of configuration interaction (CI-CSP) [20,21].

Although the CSP and CI-CSP techniques are tailored to large systems, we find it useful to apply them also to small triatomics where numerically exact calculations are still feasible. Such a test is more precise and direct than the usual checks against experiment (e.g. we can abstract the influence of the choice of the interaction potential), and therefore useful for assessing the quality of the approximate methods and for finding ways of improving them. Nevertheless, we prefer to apply and test our methods on relevant and realistic systems and processes rather than on artificial models. Therefore, we focus in this Letter on quantum vibrational dynamics following electron photodetachment in the  $\Gamma^- \text{Ar}_2$  cluster. The cryogenic  $\Gamma^- \text{Ar}_n$  ( $n = 1-19$ ) complexes have been extensively investigated using photoelectron and ZEKE spectroscopy by the group of Neumark [22,23] and were also the focus of our earlier studies [18,24]. The main goal of this work is to model this process using CSP, CI-CSP, TDSCF and numerically exact methods and elucidate the strong and weak points of the first two approximate approaches.

The Letter is organized as follows. In Section 2 we briefly review the new computational techniques. In Section 3 we give details concerning the system and the computer simulations, and in Section 4 we present and discuss the results of the quantum dynamical calculations. Finally, conclusions are to be found in Section 5.

## 2. Method

### 2.1. Classical separable potential method

The CSP method, which is the starting point for the configuration interaction extension, has been extensively described in detail elsewhere [18,21]. Briefly, the basic concept of the CSP method lies in simplifying the multidimensional coupled quantum dynamical problem by constructing an effective time-dependent separable mean-field potential for each degree of freedom using auxiliary classical trajectories. Using the ensemble of trajectories, an effective potential for each mode is computed. Subsequently, the system is ‘quantized’, and a one-dimensional quantum propagation is performed for each mode using the above separable potentials.

The set of  $n_T$  classical trajectories  $\{q_1^{(\alpha)}(t), q_2^{(\alpha)}(t), \dots, q_N^{(\alpha)}(t), \alpha = 1, \dots, n_T\}$  is started from Wigner coordinates and momenta which map the initial wavepacket. This set is then generated by solving the classical equations of motion and used to construct a separable time-dependent effective potential  $V_j(q_j, t)$  for each mode  $j$  ( $j = 1, 2, \dots, N$ ) by averaging over all trajectories in the following way:

$$V_j(q_j, t) = \sum_{\alpha=1}^{n_T} V(q_1^{(\alpha)}(t), \dots, q_{j-1}^{(\alpha)}(t), q_j, q_{j+1}^{(\alpha)}(t), \dots, q_N^{(\alpha)}(t)) w_\alpha + \frac{1-N}{N} \bar{V}(t). \quad (1)$$

Here  $V$  is the fully coupled potential,  $N$  is the number of modes, the summation runs over all MD trajectories and  $w_\alpha$  is the Wigner weight of trajectory  $\alpha$ . The coordinate-independent constant  $\bar{V}$

$$\bar{V}(t) = \sum_{\alpha=1}^{n_T} V(q_1^{(\alpha)}(t), \dots, q_{j-1}^{(\alpha)}(t), q_j^{(\alpha)}(t), q_{j+1}^{(\alpha)}(t), \dots, q_N^{(\alpha)}(t)) w_\alpha, \quad (2)$$

which does not influence the dynamics ensures that the single-mode potentials sum approximately to the total potential energy of the system.

Finally, the time-dependent Schrödinger equation in the separable approximation is solved for each mode  $j$

$$i\hbar \frac{\partial \psi_j^0(q_j, t)}{\partial t} = (\hat{T}_j + V_j(q_j, t)) \psi_j^0(q_j, t), \quad j = 1, \dots, N. \quad (3)$$

Here normal mode coordinates are used,  $2\pi\hbar$  represents the Planck's constant,  $\hat{T}_j$  is the kinetic energy operator of mode  $j$  and the upper index 0 marks the CSP level of approximation. The total wavepacket for the system under study is then given as a product of the single-mode wavefunctions

$$\Psi^0(q_1, \dots, q_N, t) = \prod_{j=1}^N \psi_j^0(q_j, t). \quad (4)$$

## 2.2. Configuration interaction extension of the CSP method

The configuration interaction (CI) based on the CSP method has been outlined recently [20,21]. The philosophy is again to use classical MD to overcome the unfavorable scaling of the computational effort with the system size. More specifically, classical trajectories, which describe fully correlated dynamics, are used to guide the selection of important CI terms and to enable the evaluation of coupling terms without highly dimensional quadratures.

First, we propagate separable wavepackets  $\Psi^{(\alpha)} = \psi_1^{(\alpha)} \times \dots \times \psi_N^{(\alpha)}$  along individual classical trajectories  $\alpha$ , i.e. using potentials of the type

$$V_j^{(\alpha)}(q_j, t) = V(q_1^{(\alpha)}(t), \dots, q_{j-1}^{(\alpha)}(t), q_j, q_{j+1}^{(\alpha)}(t), \dots, q_N^{(\alpha)}(t)) + \frac{1-N}{N} \bar{V}^{(\alpha)}(t), \quad (5)$$

together with the CSP wavepacket guided by the corresponding potentials (see Eq. 1). The coordinate-independent constants  $\bar{V}^{(\alpha)}$

$$\bar{V}^{(\alpha)}(t) = V(q_1^{(\alpha)}(t), \dots, q_j^{(\alpha)}(t), \dots, q_N^{(\alpha)}(t)), \quad (6)$$

again do not influence the dynamics and are only added for energy normalization.

The CI-CSP *ansatz* for the wavepacket is as follows:

$$\begin{aligned} \Psi(q_1, \dots, q_N, t) = & c_0 \psi_1^0 \dots \psi_N^0 + \sum_{j, \alpha}^{N, M_j} s_{j\alpha} \psi_1^0 \dots \psi_j^{(\alpha)} \dots \psi_N^0 \\ & + \sum_{j(<j'), \alpha, j', \beta}^{N, M_j, N, M_j} d_{j\alpha j'\beta} \psi_1^0 \dots \psi_j^{(\alpha)} \dots \psi_{j'}^{(\beta)} \dots \psi_N^0. \end{aligned} \quad (7)$$

Here  $\psi_j^0$  are the CSP functions and  $\psi_j^{(\alpha)}$  denote  $j$ -mode wavefunctions propagated along trajectory  $\alpha$ . These 'excited' wavefunctions are included into the CI space when the overlap between  $\psi_j^0$  and  $\psi_j^{(\alpha)}$  drops below a certain threshold (typically 95%). To make the CI problem computationally tractable the excited wavefunctions in Eq. 7 are orthogonalized with respect to the CSP wavefunctions and each other.  $N$  is the number of modes and  $M_j$  is the number of (included into the CI space) trajectories for mode  $j$ . Finally,  $c_0$  is the CSP coefficient,  $s_{j\alpha}$  are single excitation coefficients and  $d_{j\alpha j'\beta}$  are coefficients corresponding to double excitations. The familiar language of excitations is borrowed from electronic structure theory. However, in this context single excitations physically mean one-mode polarization terms and double excitations represent two-mode correlations.

Next, the CI-CSP wavepacket (Eq. 7) is substituted into the Schrödinger equation:

$$i\hbar \frac{\partial \Psi(q_1, \dots, q_N, t)}{\partial t} = \left( \sum_{j=1}^N \hat{T}_j + V(q_1, \dots, q_N) \right) \Psi(q_1, \dots, q_N, t), \quad (8)$$

where  $\hat{T}_j$  is the kinetic energy operator for mode  $j$  and  $V$  is the total (fully coupled) potential. This leads to a tractable though rather complicated set of differential equations for the time-evolution of the CI coefficients [20]. In our previous work we neglected most of the terms and took into account only the most important couplings between the CSP and doubly excited functions. Here we make a further significant step by also including couplings between individual double excitations. We have shown that there is no direct coupling between the CSP and singly excited terms [20] which is a time-dependent manifestation of the Brillouin theorem. Therefore, the influence of single excitations is only indirect (via double excitations) and should be small at least on short timescales and so we continue to neglect it in this work. The working equations at this level of approximation, which we denote CID-CSP, are as follows [20]:

$$\begin{aligned} i\hbar \frac{\partial c_0}{\partial t} &= \sum_{j(<j'), \alpha, j', \beta}^{N, M_j, N, M_j} d_{j\alpha j'\beta} \langle \psi_j^0 \psi_j^0 | V_{jj}^{\text{CSP2}} | \psi_j^{(\alpha)} \psi_j^{(\beta)} \rangle, \quad (9) \\ i\hbar \frac{\partial d_{j\alpha j'\beta}}{\partial t} &= -i\hbar \sum_{\gamma}^{M_j} d_{j\gamma j'\beta} \langle \psi_j^{(\alpha)} | \frac{\partial \psi_j^{(\gamma)}}{\partial t} \rangle - i\hbar \sum_{\gamma}^{M_j'} d_{j\alpha j'\gamma} \langle \psi_j^{(\beta)} | \frac{\partial \psi_j^{(\gamma)}}{\partial t} \rangle \\ &+ c_0 \langle \psi_j^{(\alpha)} \psi_j^{(\beta)} | V_{jj}^{\text{CSP2}} | \psi_j^0 \psi_j^0 \rangle + d_{j\alpha j'\beta} \left( \langle \psi_j^{(\alpha)} | \hat{T}_j | \psi_j^{(\alpha)} \rangle + \langle \psi_j^{(\beta)} | \hat{T}_j | \psi_j^{(\beta)} \rangle \right) \\ &+ \langle \psi_j^{(\alpha)} \psi_j^{(\beta)} | V_{jj}^{\text{CSP2}} | \psi_j^{(\alpha)} \psi_j^{(\beta)} \rangle - \sum_{k(\neq j, j')}^N \langle \psi_k^0 | V_k^{\text{CSP}} | \psi_k^0 \rangle \Big) \\ &+ \sum_{\gamma(\neq \alpha)}^{M_j} d_{j\gamma j'\beta} \left( \langle \psi_j^{(\alpha)} | \hat{T}_j | \psi_j^{(\gamma)} \rangle + \langle \psi_j^{(\alpha)} \psi_j^{(\beta)} | V_{jj}^{\text{CSP2}} | \psi_j^{(\gamma)} \psi_j^{(\beta)} \rangle \right) \\ &+ \sum_{\gamma(\neq \beta)}^{M_j'} d_{j\alpha j'\gamma} \left( \langle \psi_j^{(\beta)} | \hat{T}_j | \psi_j^{(\gamma)} \rangle + \langle \psi_j^{(\alpha)} \psi_j^{(\beta)} | V_{jj}^{\text{CSP2}} | \psi_j^{(\alpha)} \psi_j^{(\gamma)} \rangle \right) \\ &+ \sum_{\gamma(\neq \alpha), \delta(\neq \beta)}^{M_j, M_j'} d_{j\gamma j'\delta} \langle \psi_j^{(\alpha)} \psi_j^{(\beta)} | V_{jj}^{\text{CSP2}} | \psi_j^{(\gamma)} \psi_j^{(\delta)} \rangle \\ &+ \sum_{k(<j', \neq j), \gamma, \delta}^{N, M_k, M_j'} d_{k\gamma j'\delta} \langle \psi_j^{(\alpha)} \psi_j^{(\beta)} \psi_k^0 | V_{jjk}^{\text{CSP3}} | \psi_j^0 \psi_j^{(\delta)} \psi_k^{(\gamma)} \rangle \\ &+ \sum_{k(>j, \neq j'), \gamma, \delta}^{N, M_j, M_k} d_{j\gamma k\delta} \langle \psi_j^{(\alpha)} \psi_j^{(\beta)} \psi_k^0 | V_{jjk}^{\text{CSP3}} | \psi_j^{(\gamma)} \psi_j^0 \psi_k^{(\delta)} \rangle \\ &+ \sum_{k(<l, \neq j, j'), \gamma, l(\neq j, j'), \delta}^{N, M_k, N, M_l} d_{k\gamma l\delta} \langle \psi_j^{(\alpha)} \psi_j^{(\beta)} \psi_k^0 \psi_l^0 | V_{jjkl}^{\text{YCSP4}} | \psi_j^0 \psi_j^0 \psi_k^{(\gamma)} \psi_l^{(\delta)} \rangle. \end{aligned}$$

Here  $V_{jj}^{\text{CSP2}}$ ,  $V_{jjk}^{\text{CSP3}}$  and  $V_{jjkl}^{\text{CSP4}}$  represent two-, three- and four-dimensional potentials defined in analogy to the CSPs:

$$V_{jj}^{\text{CSP2}}(q_j, q_{j'}, t) = \sum_{\alpha=1}^{n_T} V(q_1^{(\alpha)}(t), \dots, q_j, \dots, q_{j'}, \dots, q_N^{(\alpha)}(t)) w_{\alpha}, \quad (10)$$

$$V_{jjk}^{\text{CSP3}}(q_j, q_{j'}, q_{j'k}, t) = \sum_{\alpha=1}^{n_T} V(q_1^{(\alpha)}(t), \dots, q_j, \dots, q_{j'}, \dots, q_k, \dots, q_N^{(\alpha)}(t)) w_{\alpha}. \quad (11)$$

$$V_{jjkl}^{\text{CSP4}}(q_j, q_{j'}, q_k, q_l, t) = \sum_{\alpha=1}^{n_T} V(q_1^{(\alpha)}(t), \dots, q_j, \dots, q_{j'}, \dots, q_k, \dots, q_l, \dots, q_N^{(\alpha)}(t)) w_{\alpha}. \quad (12)$$

The  $\langle \psi_j^0 \psi_{j'}^0 | V_{jj}^{\text{CSP2}} | \psi_j^{(\alpha)} \psi_{j'}^{(\beta)} \rangle$  terms which couple the double excitations with the CSP functions are also used as a criterion for a significant reduction of the CI space by omitting unimportant terms; namely, only those double excitations for which the absolute value of this coupling term is larger than an empirically adjusted threshold are included. The right choice of threshold must be such that the results are practically uninfluenced by it.

### 3. System and simulations

Upon electron photodetachment in the  $\text{I}^- \text{Ar}_2$  complex, which has the shape of an isosceles (nearly equilateral) triangle [23,24], the ground state vibrational wavefunction is promoted to a neutral surface where it is no longer stationary and therefore undergoes dynamical evolution. The anionic and neutral iodine–argon potentials were extracted from ZEKE experiments [22]. Here we use the same parameters and pairwise *ansatz* as in our previous work [18,24]. Out of the three possible quasidegenerate neutral states (given by the spatial orientation of the singly occupied p-orbital of the iodine atom) where the system can land upon electron photodetachment we chose for our dynamical study the second I3/2 state [22]. The potential for this state differs most from the anionic one, therefore interesting dynamics can be expected. From a technical point of view, for planar systems such as  $\text{IAr}_2$  this I3/2 state is of pure II-character. Therefore, for this state of the system under study simple pair additivity is adequate (as in the case of spherical atoms) and there is no need for more complicated diatomics-in-molecule schemes [24].

For all the simulations, the coordinates used were the anionic normal modes (symmetric and asymmetric stretch and the bending mode) and the initial wavepacket was a product of corresponding Gaussians. A grid of 32 points for each degree of freedom proved to be sufficient. The action of the kinetic energy operator was evaluated using the Fourier approach [5]. All separable wavepackets were propagated using the split-operator technique [25] with a time-step of 0.65 fs. The numerically exact wavefunction was propagated using the Chebyshev method [26] with a 6.5 fs time-step. Classical trajectories were generated using a standard Gear routine [1] and the CI coefficients were propagated using a Runge–Kutta method [27]. Converged CSP and CID-CSP results were obtained with 200 classical trajectories and 300 CI functions.

## 4. Results and discussion

### 4.1. Auto correlation functions

ZEKE spectra of small  $\text{I}^- \text{Ar}_n$  clusters exhibit vibrational structure which gradually gets washed out with increasing system size [22,23]. From a dynamical point of view distinct vibrational lines are manifestations of recurrences in the nuclear motions on the potential surface of the neutral species after electron photodetachment.

More precisely, the intensity  $I(\omega)$  of the ZEKE signal is directly connected with the autocorrelation function  $C_A(t)$  (i.e. the overlap between the total wavepacket at time  $t$  and at time 0) via the Fourier transform [28]

$$I(\omega) \sim \omega \times \int_{-} C_A(t) e^{i(E_i + \omega)t} dt, \quad (13)$$

where  $E_i$  is the initial energy of the system. It should be stressed at this point that the formulae for spectra evaluations are purely quantum mechanical and therefore require a quantum description of the dynamics. Even if the atomic motions themselves are not strongly quantal, the spectral intensities of the vibrational lines are sensitive to phase relations in the wavepacket, which can hardly be quantitatively reproduced by classical mechanics [29].

As cluster size increases, more vibrational degrees of freedom actively participate in the nuclear dynamics. Due to the stronger intramolecular vibrational redistribution (IVR) a reappearance in the overall nuclear motion becomes unlikely before dephasing of the wavepacket. As a result, there are no recurrences in the autocorrelation function and only a broad unstructured photoelectron signal is observed for large  $I^-Ar_n$  complexes [23]. Already in the  $I^-Ar_2$  cluster the washing out of the vibrational structure is strong, although a damped progression of vibrational lines corresponding to weak recurrences in the autocorrelation function on a picosecond timescale is still observable. The 1200 fs interval covered by our simulations represents one to two vibrational periods of the individual modes and the buildup of the first recurrence in the collective nuclear motion. From a methodological point of view, this time interval covers the onset of deviations of approximate treatments from the numerically exact simulation.

Due to its direct relation to observable spectra, the autocorrelation function is a key quantity in the quantum dynamical description of photochemical processes [29]. Moreover, it is at the same time a sensitive probe of the quality of approximate methods, since it is sensitive not only to the amplitude but also to the phase of the total vibrational wavepacket. For these reasons we chose it as the principal testing quantity. Fig. 1 depicts the autocorrelation functions calculated using three approximate methods – CSP, CID-CSP and TDSCF, and compares them with the numerically exact calculation. The first important result is that mean-field separable methods (CSP and TDSCF) represent a good qualitative approximation, at least on the timescale covered by our

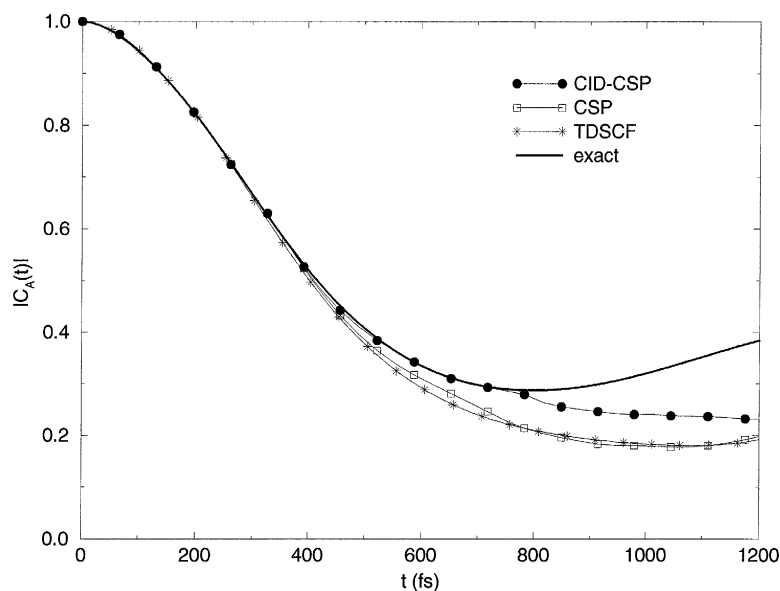


Fig. 1. Comparison between the CSP, CID-CSP, TDSCF and numerically exact autocorrelation functions.

simulations. This is true despite the fact that the complex under study is not an ideal case for separable approaches, since it lacks significant separation in the frequencies of the individual vibrational motions. The second important result is the excellent agreement between the CSP and TDSCF autocorrelation functions, which indicates that approximating the TDSCF integrals by weighted averages over classical trajectories is justified. Quantitatively, the mean-field results start to deviate from the exact ones around 350 fs. The inclusion of correlations via the CID-CSP method prolongs twice the nearly perfect accord with exact calculation to 700 fs. Even after that the CID-CSP autocorrelation function remains significantly better than the CSP one. This shows that the CID-CSP approach, which can, be principle, in pushed closer and closer to the exact limit by the inclusion of single and higher than double excitations, substantially improves the separable CSP results.

It is important to stress that the good performance of approximate methods cannot be attributed to weak couplings between the vibrational modes. On the contrary, the couplings in the system under study are relatively strong, especially between the symmetric stretch and the bending mode. This is clearly demonstrated in Fig. 2 where the CSP autocorrelation function is compared with that following from a calculation with ‘switched off’ couplings. Such a result is obtained by not updating the CSP potentials during the simulation, i.e. freezing them at  $t=0$ . Due to the lack of intermode couplings this artificial autocorrelation function starts early to qualitatively deviate from the CSP one (and the numerically exact one as well), and becomes meaningless. We should note here that unlike the ‘real’  $\text{IAr}_2$  cluster the system with ‘switched off’ couplings does not directly correlate with any experimental reality. However, it allows us to get a feeling about the strength of the intermode couplings in the ‘real’ system and about the quality of the approximate approaches.

The principal idea of the CSP method is to replace the computationally tedious and for large systems hardly doable multidimensional TDSCF integrals by weighted averages over classical trajectories. In this we are taking advantage of the fact that a swarm of classical trajectories starting from proper initial conditions [29] is often a good representation of the quantum wavepacket in cases where the phase information plays no role, as in the evaluation of effective mean-field potentials. However, why do we not simply approximate the above ‘bottleneck’ integrals using the value of the integrand at the peak of the wavepacket or, in the classical language, by the value of the potential along a central trajectory starting at the top of the Wigner distribution?

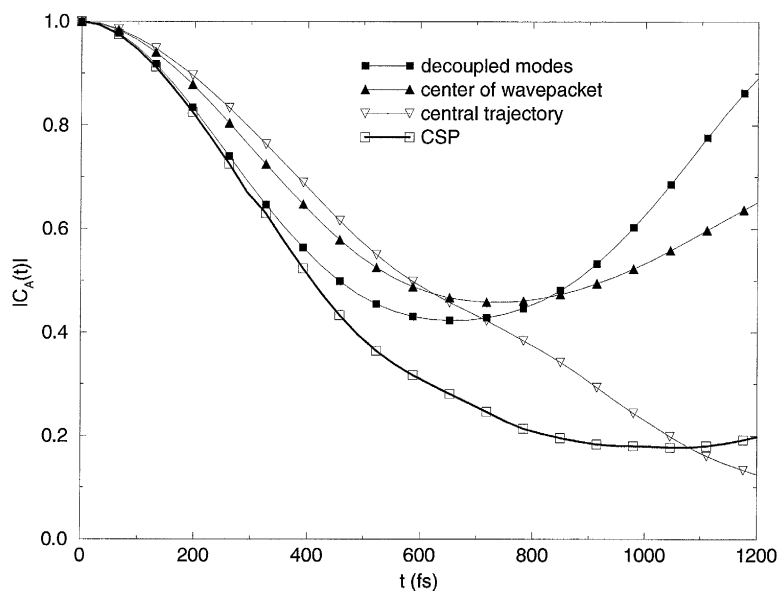


Fig. 2. Autocorrelation functions using ‘decoupled’ modes, center of the wavepacket and the central trajectory in comparison with the CSP result.

The answer to this question is demonstrated again in Fig. 2. Autocorrelation functions calculated using just the peak of the wavepacket or the central trajectory, are even worse than the ‘uncoupled’ result, and are clearly unsatisfactory. The conclusion is that we cannot afford to neglect the width and the shape of the vibrational wavepacket if we wish to accurately reproduce the dynamics and spectra.

#### 4.2. Wavepackets and overlaps

For graphical visualization we chose to show only the symmetric stretch mode which is, due to its character and the shape of the potential surfaces, mostly involved in the dynamics and couplings. In the case of separable wavepackets it is possible to directly show the single mode function; for non-separable methods it is necessary to first integrate out the remaining two degrees of freedom. Fig. 3 depicts three snapshots from the time-evolution of the symmetric stretch wavepacket together with the corresponding mean-field CSP and TDSCF potentials. Qualitatively, all the approximate methods perform well. Quantitatively, we observe a gradual deterioration of the separable wavepackets in time, the agreement between the CSP and TDSCF methods remaining good. The inclusion of correlations via CID-CSP broadens the vibrational wavepacket and brings it closer to the numerically exact one.

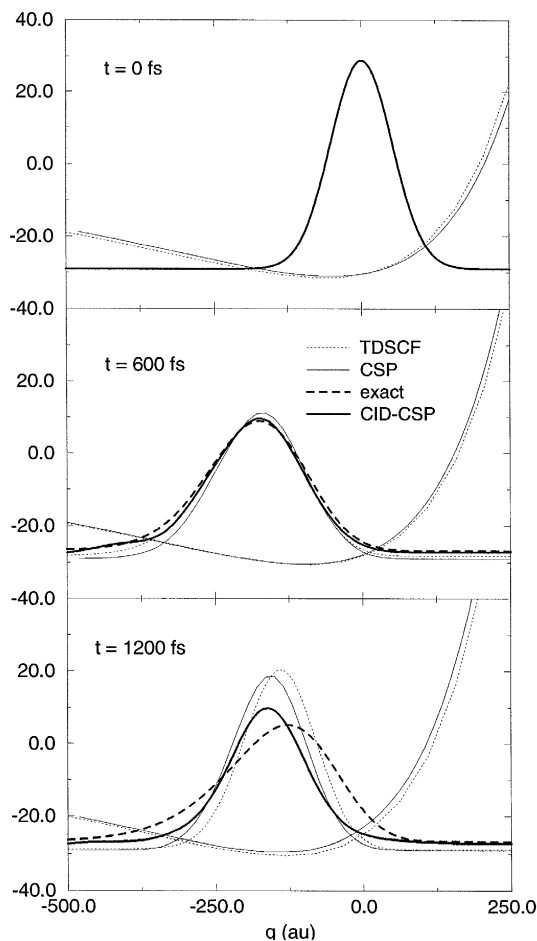


Fig. 3. Time evolution of the symmetric stretch wavepacket. Comparison between the CSP, CID-CSP, TDSCF and the numerically exact methods. Also shown are the CSP and TDSCF effective potentials for the symmetric stretch mode.

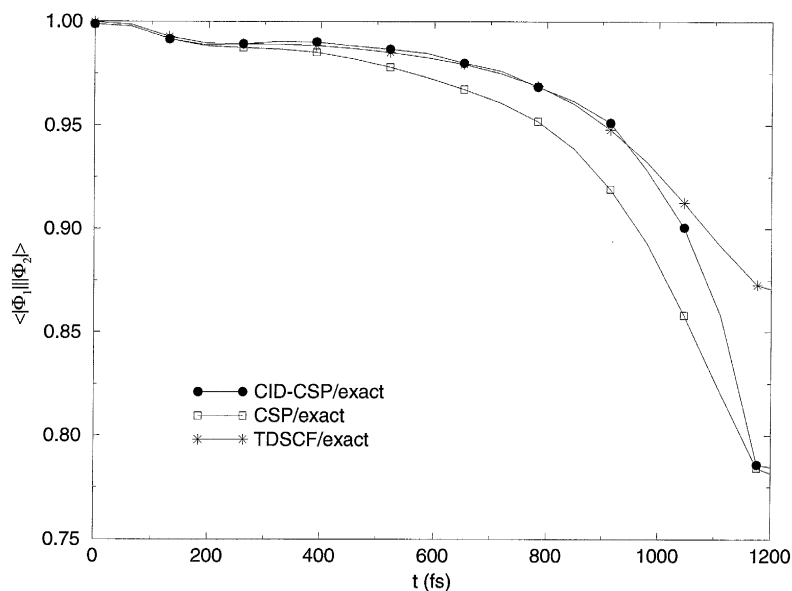


Fig. 4. CSP/exact, CID-CSP/exact and TDSCF/exact overlaps of the total wavepacket amplitudes.

Another important quantity in assessing the performance of different methods is the overlap between the approximate and numerically exact wavepackets. It is possible to plot either the amplitude of the overlap or the overlap of the wavepacket amplitudes, the latter being always closer to unity. Fig. 4 depicts the overlap between the CSP, CID-CSP, TDSCF and numerically exact total wavepacket amplitudes. It can be seen that all the approximations do well initially with the overlap dropping to 80–90% at the onset of the first recurrence at 1200 fs. Classical approximation of the TDSCF integrals results only in a minor deterioration of the CSP/exact overlap, compared to the TDSCF/exact one. Interestingly, the CID-CSP results deteriorate below the TDSCF one around 1 ps, which is probably a consequence of the neglect of single excitations. The single excitations will be explicitly included in future studies. It can also be seen from Fig. 4 that moving from the CSP to the CID-CSP method significantly improves the overlap.

## 5. Conclusions

In this work we studied the early dynamics following electron photodetachment in the  $I^-Ar_2$  complex using three approximate and the numerically exact quantum dynamical methods. On testing the quality of the new CSP and CID-CSP methods, the principal advantage being that they are also applicable to large polyatomic systems, we showed mainly that:

- (i) mean-field methods perform well on a picosecond timescale even for relatively strongly coupled systems without good separation of vibrational frequencies;
- (ii) in moderately quantal systems such as the complex under study classical trajectories can be used within the CSP method to quantitatively approximate multidimensional quantum TDSCF integrals;
- (iii) the inclusion of intermode correlations via the CID-CSP method significantly improves the approximate wavepacket bringing it closer to the numerically exact one.

## Acknowledgements

We wish to thank Professor R.B. Gerber, who is a co-author of the new quantum dynamical methods, for many stimulating discussions. This project is supported by a Volkswagen Stiftung grant No. I/72114. Partial support via grant No. A4040706 from the Granting agency of the Academy of Sciences of the Czech Republic (to PJ) is also gratefully acknowledged.

## References

- [1] M.P. Allen, D.J. Tildesley, *Computer Simulation of Liquids*, Clarendon Press, Oxford, 1987.
- [2] R.M. Whitnell, K.R. Wilson, *Reviews in Computational Chemistry*, Vol. 4, VCH, New York, 1993.
- [3] D. Kosloff, R. Kosloff, *J. Comput. Phys.* 52 (1983) 35.
- [4] R. Kosloff, D. Kosloff, *J. Chem. Phys.* 79 (1983) 1823.
- [5] R.B. Gerber, R. Kosloff, M. Berman, *Comput. Phys. Rep.* 5 (1986) 59.
- [6] C. Leforestier, R.H. Bisseling, C. Cerjan, M.D. Feit, R. Friesner, A. Gulberg, A. Hammerich, G. Jolicard, W. Karrlein, H.-D. Meyer, N. Lipkin, O. Roncero, R. Kosloff, *J. Comput. Phys.* 94 (1991) 59.
- [7] R. Kosloff, *Annu. Rev. Phys. Chem.* 45 (1994) 145.
- [8] J.C. Light, in: *Time Dependent Quantum Molecular Dynamics*, J. Broeckhove, L. Lathouwers (Eds.), Plenum Press, New York, 1992.
- [9] P.A.M. Dirac, *Proc. Cambridge Philos. Soc.* 26 (1930) 376.
- [10] R.B. Gerber, V. Buch, M.A. Ratner, *J. Chem. Phys.* 77 (1982) 3022.
- [11] R.B. Gerber, M.A. Ratner, *Adv. Chem. Phys.* 70 (1988) 97.
- [12] N. Makri, W.H. Miller, *J. Chem. Phys.* 87 (1987) 5781.
- [13] H.-D. Meyer, U. Manthe, L.S. Cederbaum, *Chem. Phys. Lett.* 165 (1990) 73.
- [14] U. Manthe, H.-D. Meyer, L.S. Cederbaum, *J. Chem. Phys.* 97 (1992) 3199.
- [15] Z. Kotler, E. Neria, A. Nitzan, *Comput. Phys. Commun.* 63 (1991) 243.
- [16] J. Campos-Martinez, R.D. Coalson, *J. Chem. Phys.* 93 (1990) 4740.
- [17] A.D. Hammerich, R. Kosloff, M.A. Ratner, *Chem. Phys. Lett.* 171 (1990) 97.
- [18] P. Jungwirth, R.B. Gerber, *J. Chem. Phys.* 102 (1995) 6046.
- [19] P. Jungwirth, E. Fredj, R.B. Gerber, *J. Chem. Phys.* 104 (1996) 9332.
- [20] P. Jungwirth, E. Fredj, R.B. Gerber, *J. Chem. Phys.* submitted.
- [21] R.B. Gerber, P. Jungwirth, E. Fredj, A.Y. Rom, in: *Multidimensional Molecular Dynamics Methods*, D.L. Thompson (Ed.), World Scientific, River Edge, NJ, 1997.
- [22] Y. Zhao, G. Reiser, I. Yourshaw, C.C. Arnold, D.M. Neumark, *J. Chem. Phys.* 101 (1994) 6538.
- [23] I. Yourshaw, Y. Zhao, D.M. Neumark, *J. Chem. Phys.* 105 (1996) 351.
- [24] P. Jungwirth, R.B. Gerber, *J. Chem. Phys.* 102 (1995) 8848.
- [25] M.D. Feit, J.A. Fleck Jr., A. Steiger, *J. Comput. Phys.* 47 (1982) 412.
- [26] H. Tal-Ezer, R. Kosloff, *J. Chem. Phys.* 81 (1984) 3967.
- [27] W.H. Press, S.A. Teukolsky, W.T. Vetterling, B.P. Flannery, *Numerical Recipes in Fortran*, Cambridge University Press, Cambridge, 1992.
- [28] E.J. Heller, *Acc. Chem. Res.* 14 (1981) 368.
- [29] R. Schinke, *Photodissociation Dynamics*, Cambridge University Press, Cambridge, 1993, pp. 72–108.